GENERAL ELECTRIC CO.
Missile and Space Division
Space Sciences Laboratory
P. O. Box 8555
Philadelphia, Pa. 19101

Fifth Quarterly Progress Report

STUDY OF PARAMETRIC PERFORMANCE OF A TWO-STAGE REPETITIVELY PULSED PLASMA ENGINE (REPPAC)

B. Gorowitz P. Gloersen T. Karras

Contract NASw-1044

November 5, 1965

Prepared For: National Aeronautics and Space Administration

Lewis Research Center

Cleveland, Ohio

TABLE OF CONTENTS

LIST OF FIGURES

1. INTRODUCTION

During the period covered by this report, two significant changes were made in portions of the engine system; the original capacitor bank was replaced by units of higher Q resulting in greater energy transfer to the gun and the propellant valve seat was redesigned to provide better control over the propellant distribution. Calorimetric measurements of the exhaust stream indicated peak energy efficiencies of 77% at a capacitor voltage of 2 KV, (taking into account the Q of the new bank) while thrust and mass flow measurements at the same voltage indicated peak overall efficiencies of 70% at an I_{sp} of 9500 sec and an efficiency of 50% at 6000 sec.

Some initial measurements of ion velocities were made using the multigridded electrostatic probe. The deduced I_{sp}'s were in close agreement with those obtained from the $T/\dot{m}\,g$ calculations.

Fast ion gauge probe measurements of the neutral propellant density distribution indicated that the placement of propellant had been sharply altered to provide a more axial stream than had been previously obtained with high conductance nozzles. It was determined that over 90% of the initially injected propellant mass was available for use at the time the discharge was triggered.

In preparation for longer term operation of the engine at the 2 KW level, runs were carried out for periods of up to 45 minutes duration. Exhaust stream energies measured by the calorimeter on a continuous basis were little changed in the course of any single run. Difficulties encountered due to the heating of fast-acting valve components were largely eliminated, pointing the way to tests of considerably longer duration.

2. NEW CAPACITOR BANK

During the most recent quarterly period, the nine units of the

original paper-oil dielectric 45 μfd capacitor bank were replaced by an equal number of dry type mylar dielectric units arranged in an array of 3 modules, each containing three capacitors of 5 μfd nominal capacitance and 2.5 KV rating. One such module is shown in Figure 1. The total capacitance possible by filling the module shown is 25 μfd. By using 9 such modules in place of the original capacitors which were mounted on the same parallel plate aluminum flanges, the bank capacitance can be increased to 225 μfd. The Q of the new 45 mfd bank, measured at 100 KC ringing frequency, is 14, twice that of the old installation. As will be shown later, the change in capacitors resulted in an increase in energy efficiency greater than that expected entirely on the basis of the different Q's. The various efficiencies presented have taken into account capacitor losses, and it appeared that in spite of this, there was an increase in the peak values of energy efficiency observed from 72% to 77%. The reason for this increase is not yet completely understood. It cannot be explained on the basis of unaccounted for changes in the inductance or capacitance of the system. The total inductance of the system has been changed only slightly by the new capacitors, since the header and gun flanges represent by far the greatest portion of the inductance. The capacitance of the bank was measured and found to be 42.5 μfd instead of the nominal value of 45 μfd. This new lower capacitance was taken into account in the calculations of energy input. More detailed investigation of the current and voltage signals at the gun terminals may provide a better indication of the actual changes in energy transfer to the gun.

3. REDESIGNED VALVE SEAT - GAS DENSITY PROBE MEASUREMENTS

3.1 Introductory Remarks

It was pointed out in the last quarterly report that an attempt would be made to devise a technique for redirecting the flow of the propellant stream by changes in the valve seat. The motivation for this goal arose from measurements performed on the A 9D gun that showed the bulk of the

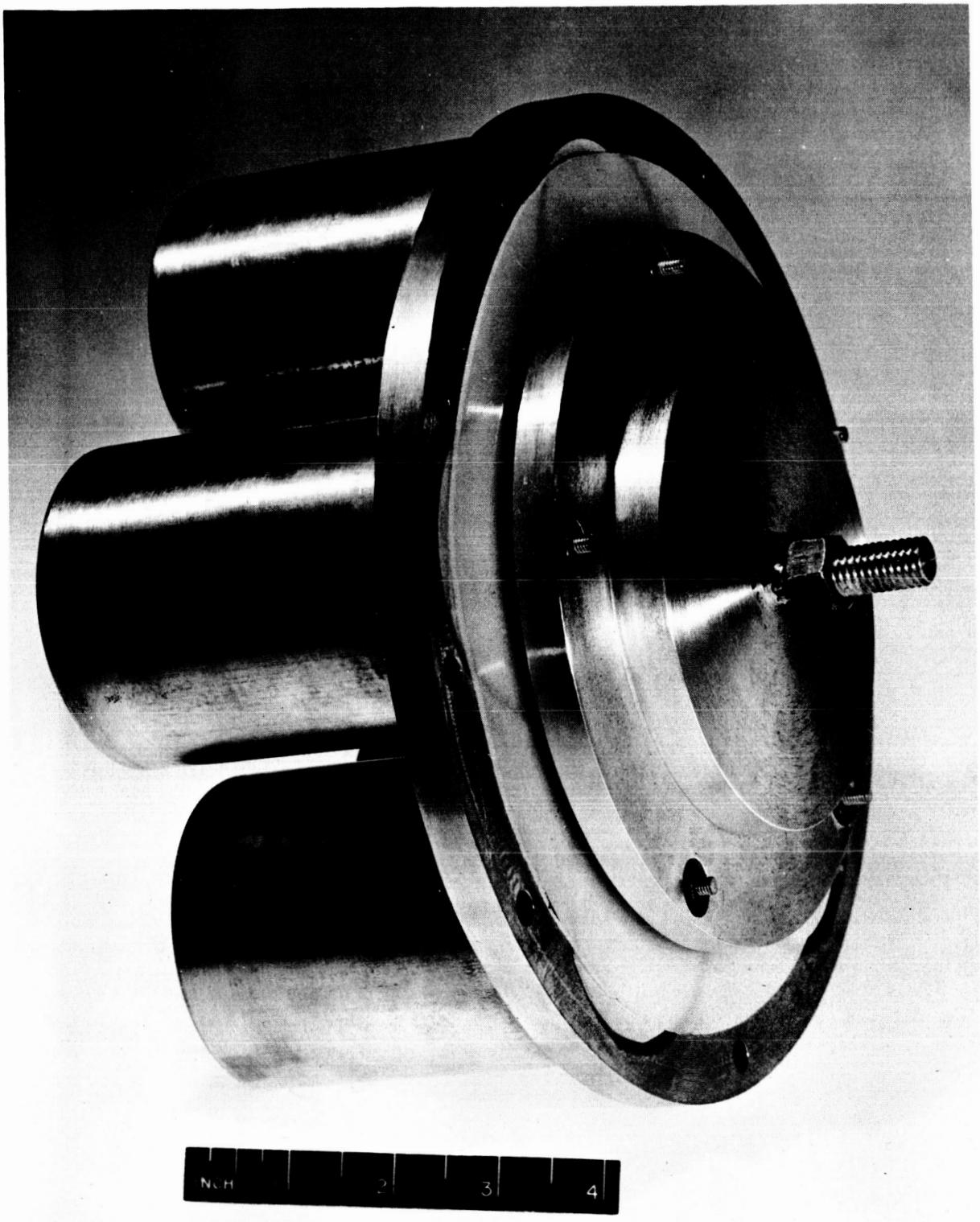

Figure 1. Capacitor Module

gas flow moving directly to the outer electrode[1]. As a result, self-triggering occurred very early and with undesirably small amounts of injected propellant, drastically limiting the amount of propellant that could be used in triggered operation. In addition, the positioning of the propellant in a region of low field strength also seemed undesirable. The drop in efficiency observed from performance measurements on the A9D gun tended to verify this and fit in with the view that a more axial flow must be given to the propellant. Redesign of the fast-acting valve seat provided a means for controlling the propellant distribution in the gun without changing the shape of the center electrode. The new valve seat, drawn in Figure 11a, consists of a teflon "O" ring mated with a stainless steel ball which is of appropriate diameter with relation to the I. D. of the "O" ring to control the axiality of the propellant flow, i. e., the most pronounced axial flow is obtained when the ball diameter is closest to the "O" ring I. D. Propellant distribution measurements using the CK5702 ion gauge probe were made for one such valve seat installed in the A-9 and A-8 nozzle geometries. (The series of guns using the ball seat valve are henceforth designated with a "B" suffix, i. e., A-9DB and A-8DB.)

3. 2 A9DB Results

An initial crude study was performed on the A9DB configuration until it became clear that the more efficient A-8DB would be used rather than the A9DB for the more extensive performance measurements to follow.

By chance, the isobars for the A9DB were obtained on a plane a little off axis and so did not unambiguously show the high density stream against the central electrode as expected. Nonetheless, the general pattern (see figures 2 and 3) very strongly suggested such a position for the high density stream. The absence of the stream in any other location also tended to confirm that position. A detailed discussion of this will

---

1. 4th Quarterly Progress Report - NASA Contract NASw-1044 - 1965

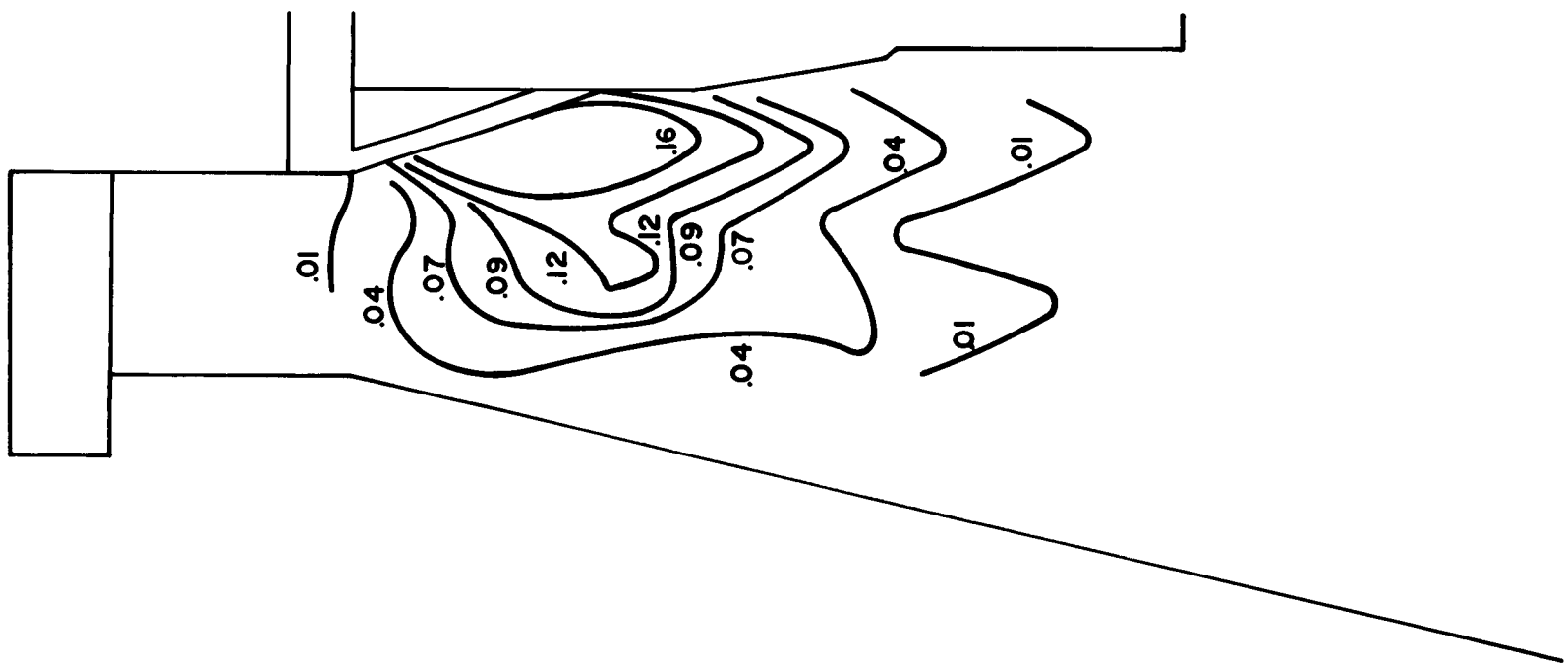

Figure 2. A-9DB Propellant Distribution at .5 ms.

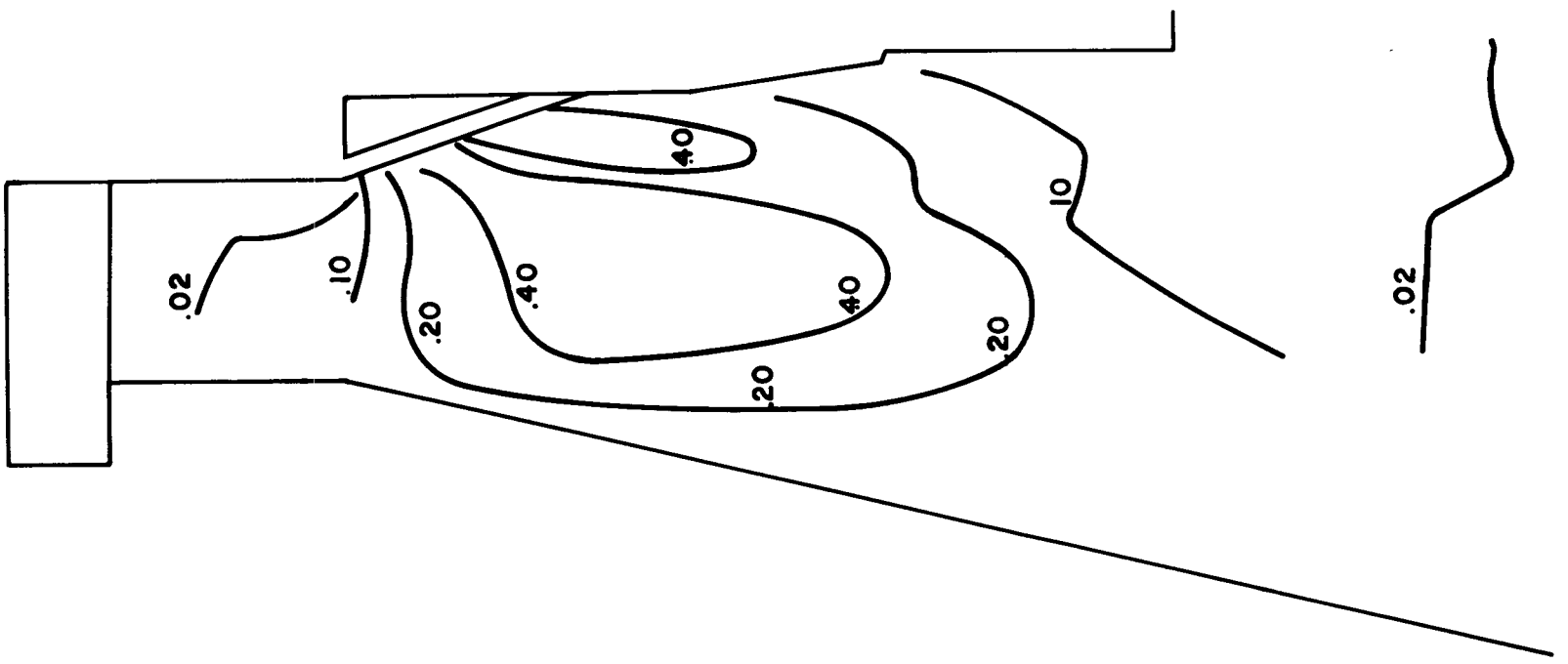

Figure 3. A-9DB Propellant Distribution at .8 ms.

be carried out in the next section covering the A8DB gun.

Due to the new valve seat, there arose the question of the symmetry of propellant injection. This symmetry can be tested by examining the pressure along two lines parallel to the axis and symmetrically placed in respect to that axis (taken at times a day apart) as is shown on Figure 4. While by no means identical, these curves are of the same general level and shape, indicating a reasonably symmetric propellant injection. In addition, the repeatability of the pressure vs. time traces (without which construction of isobars would be impossible) indicates the repeatability of the quantity of gas admitted.

3.3 A8DB Results

Performance measurements carried out at this time on the A8DB gun indicated sufficiently high efficiencies to warrant detailed gas density measurements.

A gun which had been consistently giving calorimetrically obtained efficiencies of over 72% was separated from its outer electrode and installed in the gas density measuring facility with an identical outer electrode. Since the entire center electrode assembly was moved, the propellant injection apparatus was the same as that just used to fire the gun for the performance measurements. After the gas density measurements were over the center electrode assembly was replaced in its original position and efficiency measurements were made again. Once more, energy efficiencies of over 72% were obtained, indicating that the propellant injection system had been operating in an optimum manner during the gas density measurements.

Isobaric charts showing lines of constant pressure within the gun at succeeding times are shown in Figures 5 through 10. These contours were computed in the same way as those discussed previously[2].

In contrast to the almost radial high density stream coming from the A9D gun, here the stream enters purely axially. It runs parallel to the

---

2. 3rd Quarterly Progress Report - NASA Contract NASw-1044 - 1965.

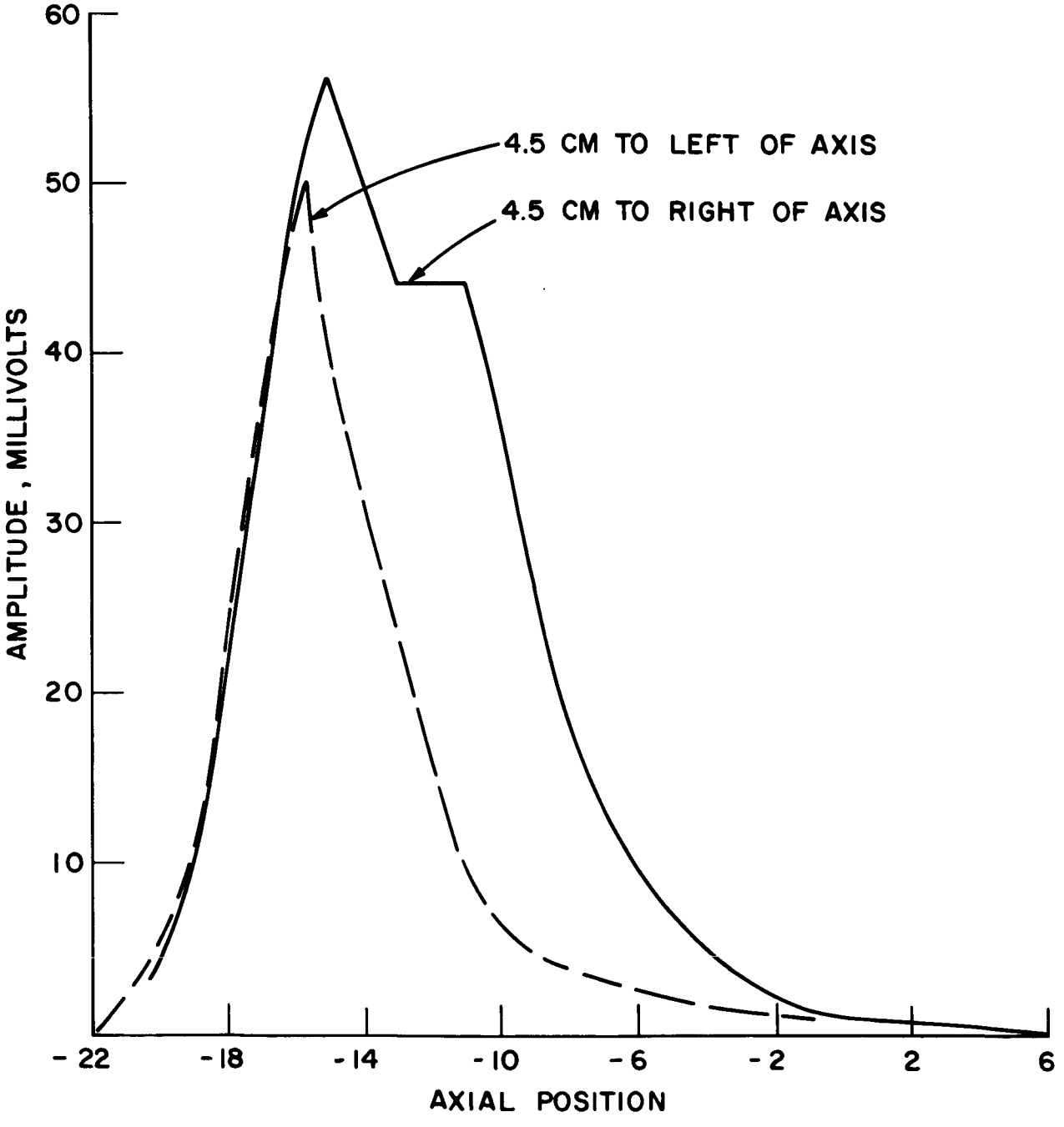

Figure 4. A-9DB Propellant Distribution along Two Symmetrically Spaced Paths at .8 ms.

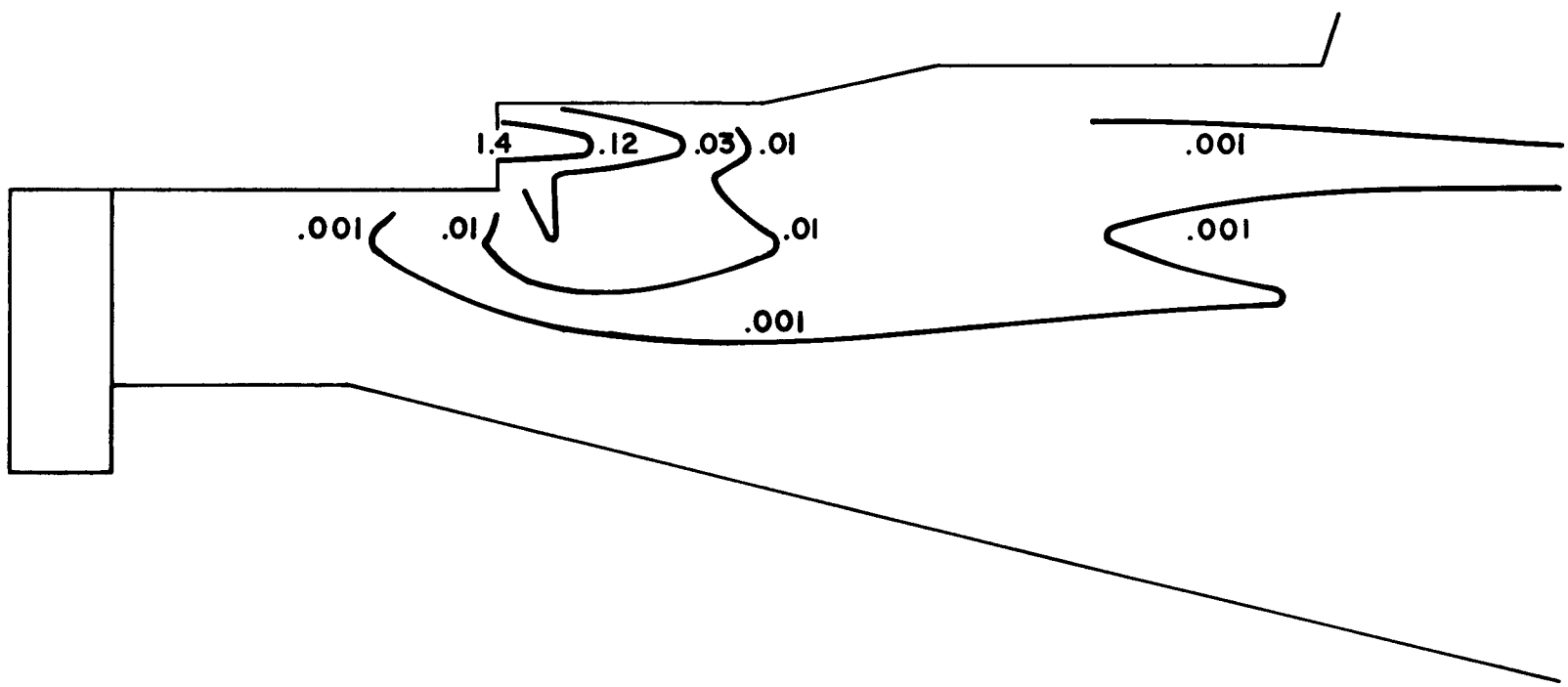

Figure 5. Isobars, A-8DB Gun at .3 ms.

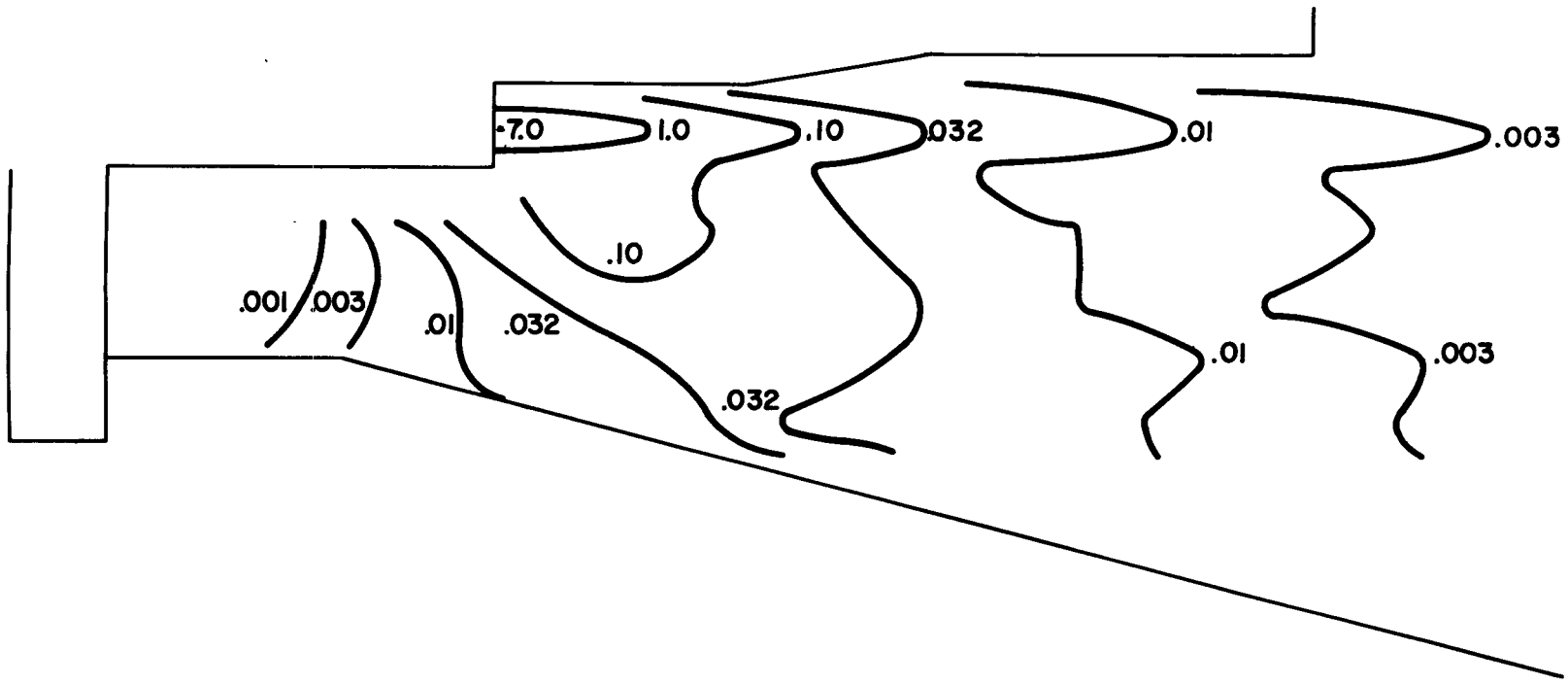

Figure 6. Isobars, A-8DB Gun at .5 ms.

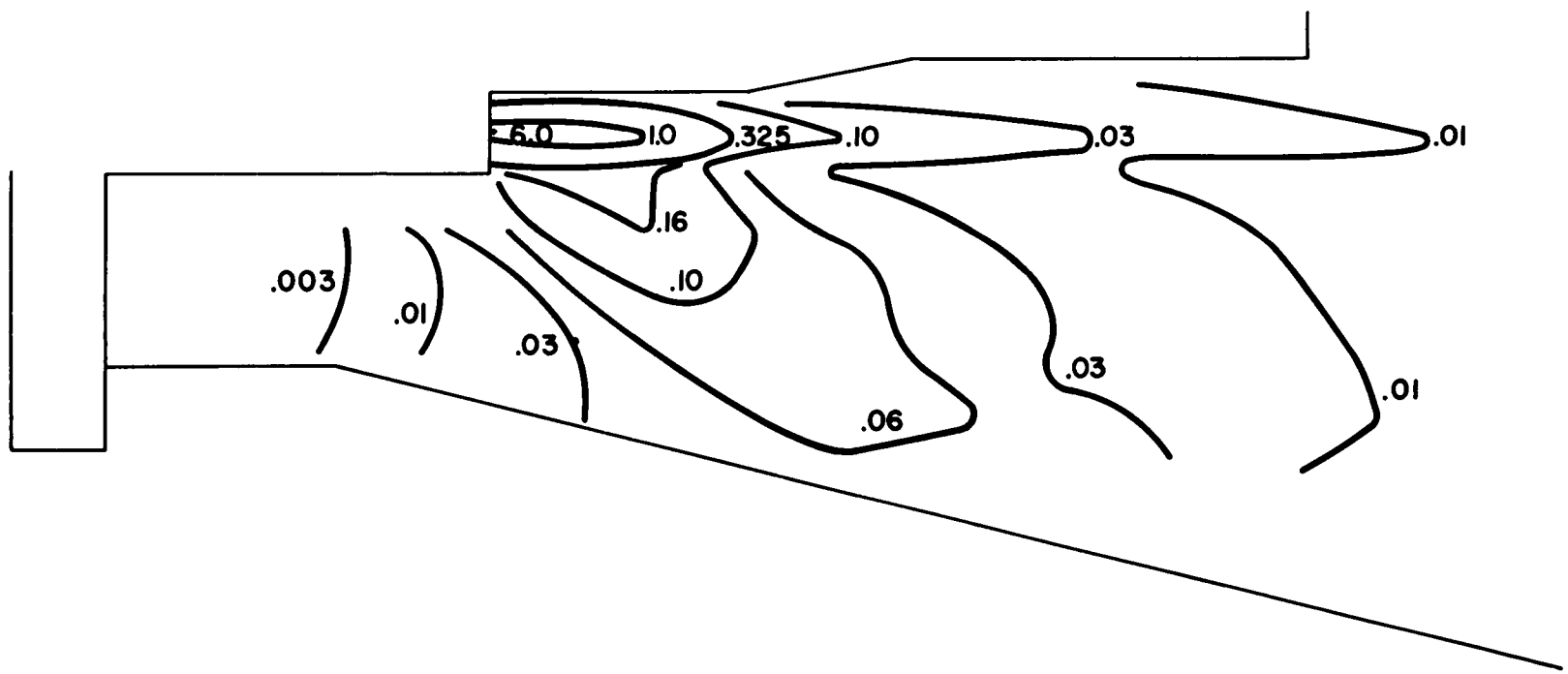

Figure 7. Isobars, A-8DB Gun at .6 ms.

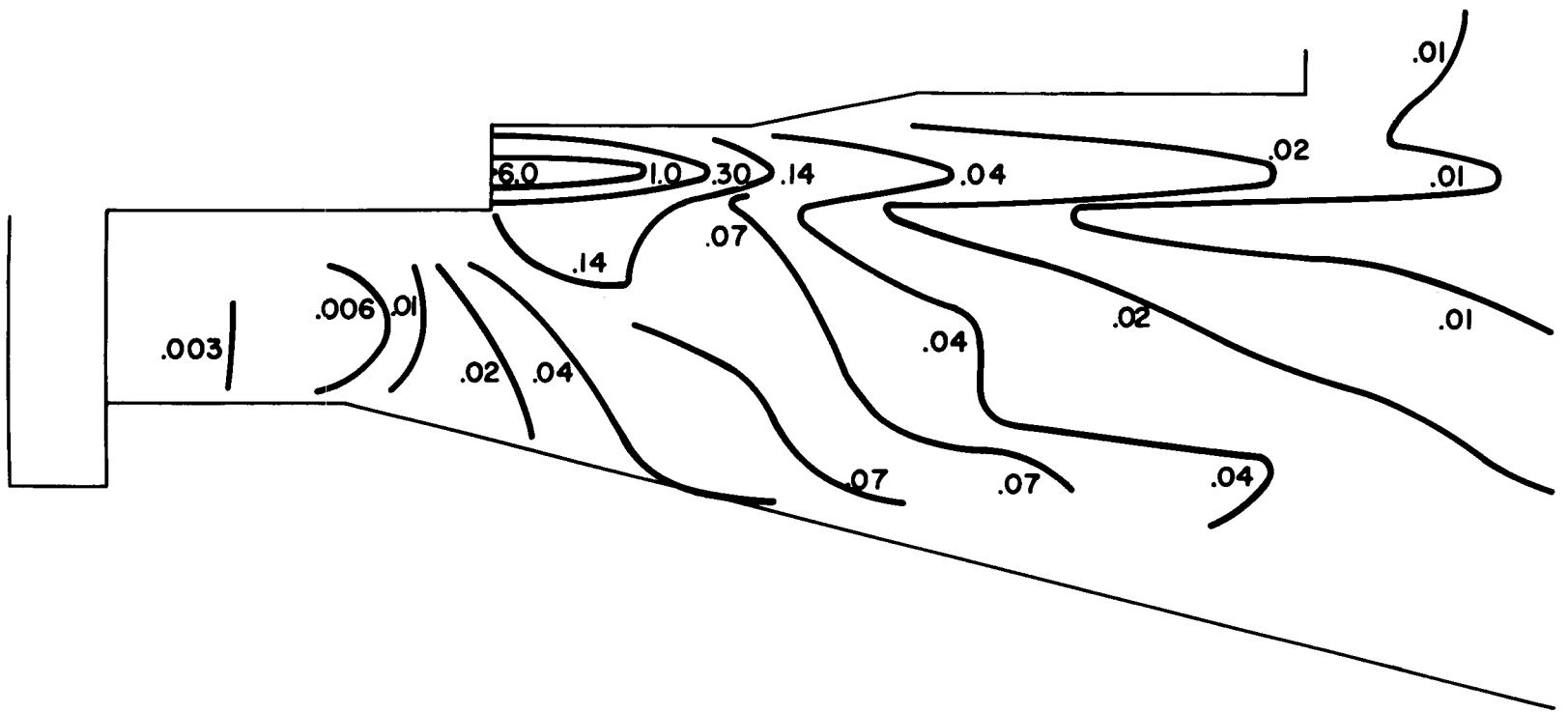

Figure 8. Isobars, A-8DB Gun at .7 ms.

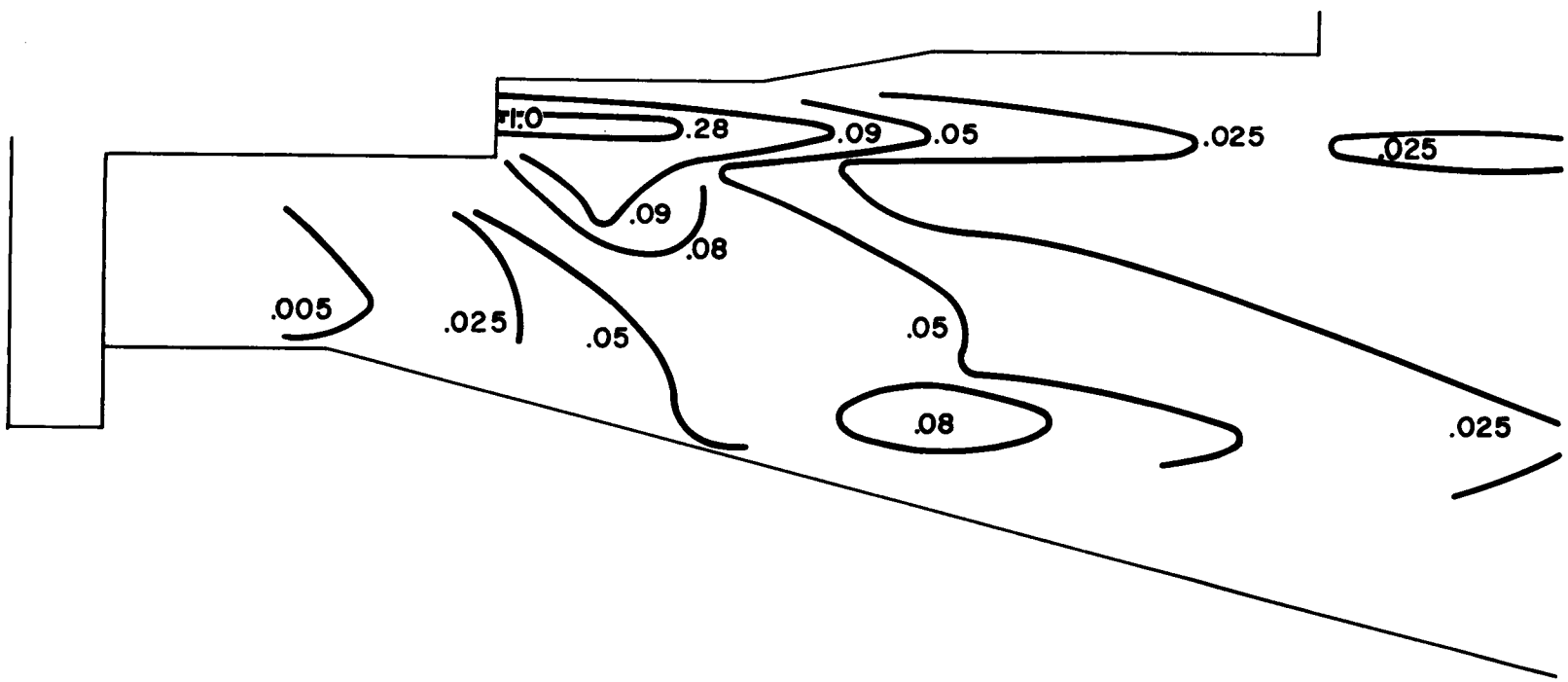

Figure 9. Isobars, A-8DB Gun at .8 ms.

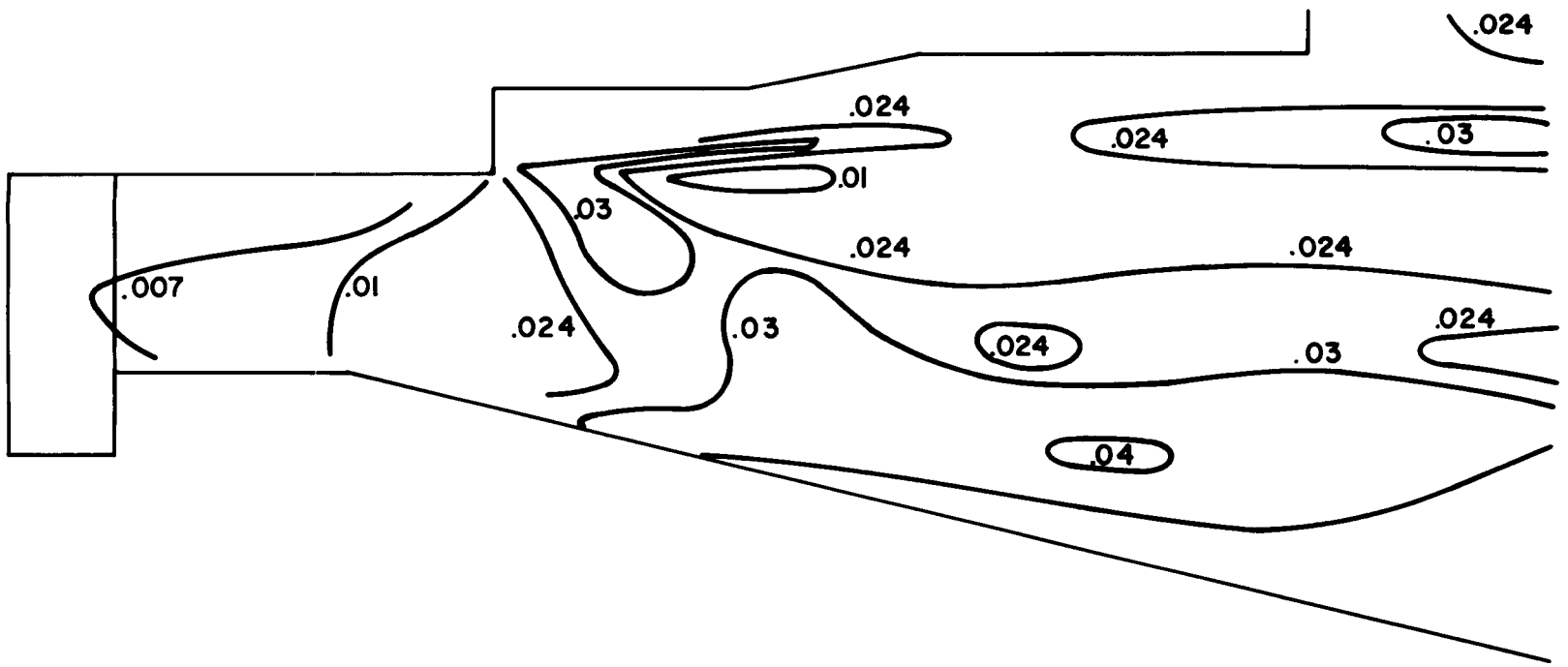

Figure 10. Isobars, A-8DB Gun at 1.0 ms.

center electrode and near the nozzle it is so narrow that radial movement of the probe by only 1/2 cm results in a drop in pressure of more than an order of magnitude. Thus, the hopes that the new valve design would provide more axial flow were completely satisfied. In addition there is a strong indication that an enlarged sphere with the same O-ring will yield a stream that makes a slight angle with the gun axis. The flat disc used previously corresponds to a sphere of infinite radius and so the angle that its stream makes with the axis should be considered as the limit one could obtain. Figure 11 (a) schematically shows the valve seat and propellant stream obtained in the A8DB gun. Figure 11 (b) and 11 (c) show the stream direction for a flat disc (infinite radius) and a sphere of intermediate radius. If it is desired, the propellant stream may be channeled in any direction using this technique.

The ability to direct the high density stream purely axially does not imply that gas can be kept away from the outer electrode to an equal degree. As can be seen in Figures 5 through 10, the high density stream develops a low density wing that moves to the outer electrode. This wing, like the main stream in the A9D gun, makes an angle of about 50° with the gun axis. There is nothing to direct the gas in this direction other than the electrode wall itself, and so the low density wing must be interpreted as the natural sidewards expansion of the high density stream.

A completely axial stream injected from the present nozzle position will give the largest fraction of propellant that can be obtained near the center electrode, and so, despite this large amount of propellant expansion toward the outer electrode, the A8DB represents the optimum gun for propellant loading in that location. No alteration in the stream position can be expected to change this situation. A nozzle with a much higher length over diameter ratio might conceivably increase the center electrode loading but the decreased nozzle conductance would more than compensate.

It should be noted here that the A9DB configuration, while having

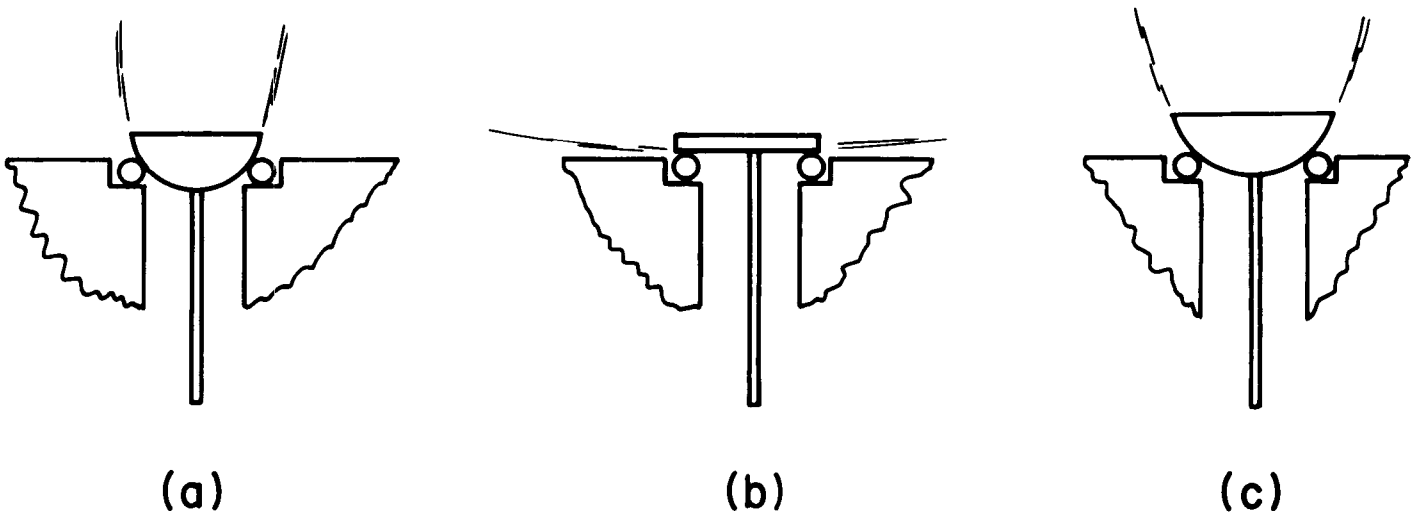

Figure 11. Sketches of Valve Seats

higher conductance, did not yield a propellant distribution significantly different from the A8DB (compare Figures 2 and 6, and 3 and 8, while noting that the A9DB data were obtained on a plane off axis.) The A9DB difficulties were probably due to the accessibility of its valve seat to the discharge and not to any deficiencies of the propellant distribution.

The above discussion is, of course, based upon the expectation that a large fraction of the propellant should be near the center electrode for efficient operation. If, for hitherto unexplored reasons, another propellant location is more desirable, changes can be made in the direction of the propellant stream to achieve such propellant positioning.

One indication of a need for this is the observation that the outer electrode becomes quite hot during extended operation with the A8DB, while the center electrode remains cool. Previous guns had left the outer electrode cold. Since the relative decrease of gas near the outer electrode is a prime characteristic of the A8DB it is possible that a slight increase in the pressure near the outer electrode would result in both electrodes running cool. Any electrode heating is an engine inefficiency and so improved performance could result.

In addition to the gross observation of the axial high density stream and its expansion into the interelectrode region, more detailed comments are possible. First, the gun is now more completely filled than in previous valve configurations. Examination of Figure 7 and 18 in references 1 and 2 show that the region around the central electrode was almost completely devoid of propellant. In fact, a pressure drop of two orders of magnitude was observed. This is not the case for either the A8DB or the A9DB guns. The pressure drop between any point on the anode and a point opposite it on the cathode is rarely more than a factor of four (except at the feed nozzles). It is not certain that this is necessarily desirable but intuition would indicate that a more uniform discharge without spokes would be likely.

A more definite benefit arises from the postponement of gun triggering. It has been noted earlier[3] that self-triggering seems to occur when an isobar of a certain density hits the outer electrode. For xenon propellant and a CK4702 tube forming the ion gauge, this isobar has been represented by .03 volts. Table 1 shows the self-triggering time and the approximate time of arrival of the .03 isobar at the outer electrode.

TABLE 1

Gun	Self-Triggering Time - ms	Approximate time of .03 isobar arrival -ms
A9D	.220	.250
A7D	.500	.475
A8DB	.550	.525
A9DB	.500	.500

Clearly, self-triggering has been delayed considerably in the A8DB and the A9DB gun configurations, and all evidence points to the more axial propellant flow as the cause. This effect was anticipated as was the greater flow required to induce self-triggering (see section 5).

To further understand the detailed effects of this mode of propellant injection, it is necessary to know what fraction of the propellant can be acted upon as a function of time. This has been computed in the same way as it was for the A7D[1] and the A9D[2]. Figure 12 shows the fraction of the propellant that is present between the feed nozzles and the muzzle as a function of time. Since gun currents extend beyond the muzzle[1], similar computations were made for the fraction of propellant between the feed nozzle and two planes 5.5 cm and 10.5 cm beyond the muzzle. The later plane represents the farthest extension of measurable currents and the other the farthest extension of significant thrust density (J x B). Figures 13 and 14 show the result of these last two computations.

---

3. T. Karras, B. Gorowitz and P. Gloersen, "Neutral Mass Density Measurements in a Repetitively Pulsed Coaxial Plasma Accelerator."Paper #65-341, AIAA Second Annual Meeting, San Francisco, California/ July 26-29, 1965.

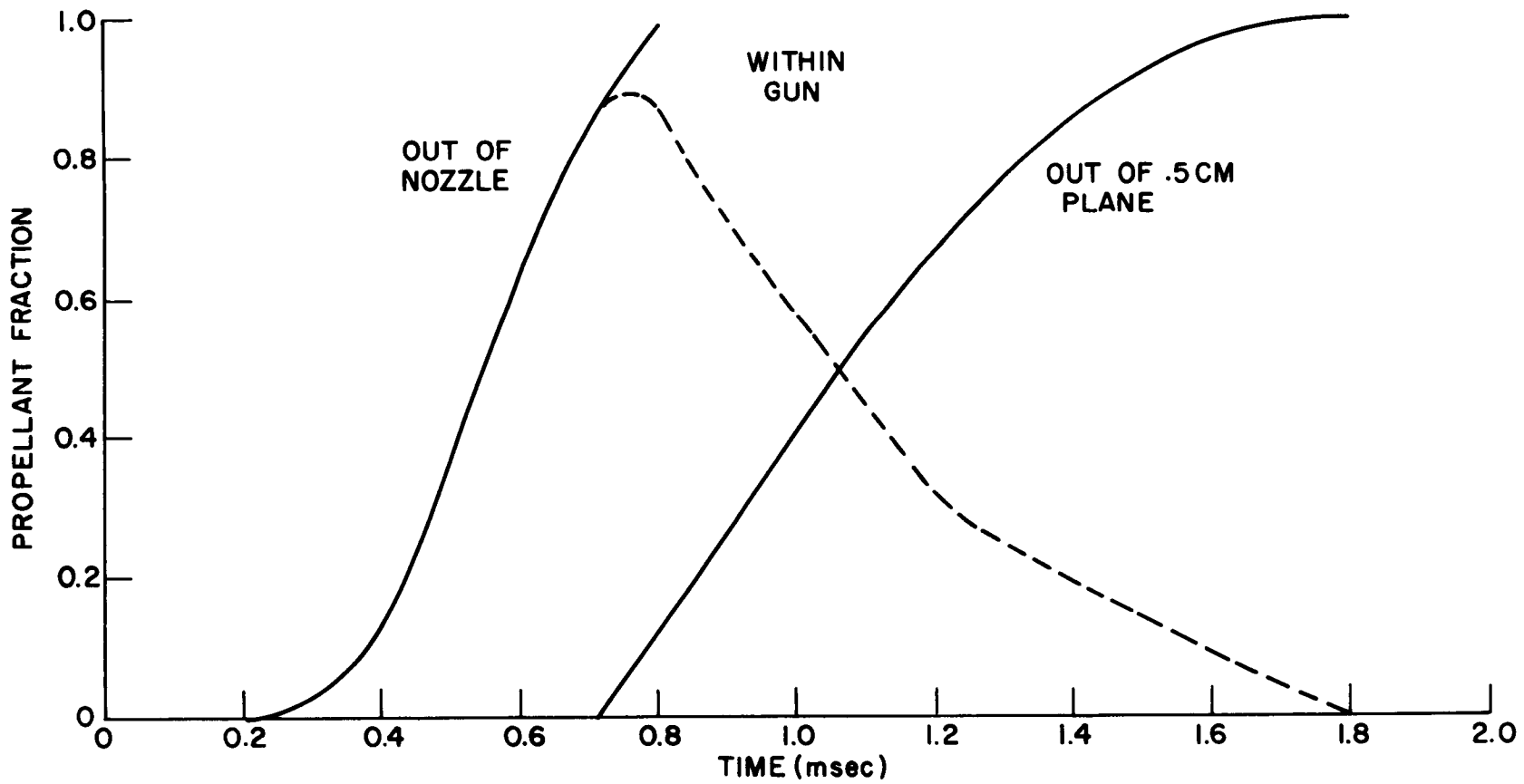

Figure 12. Propellant Fraction Between Nozzles and muzzle as a Function of Time - Axial Position = .5 cm.

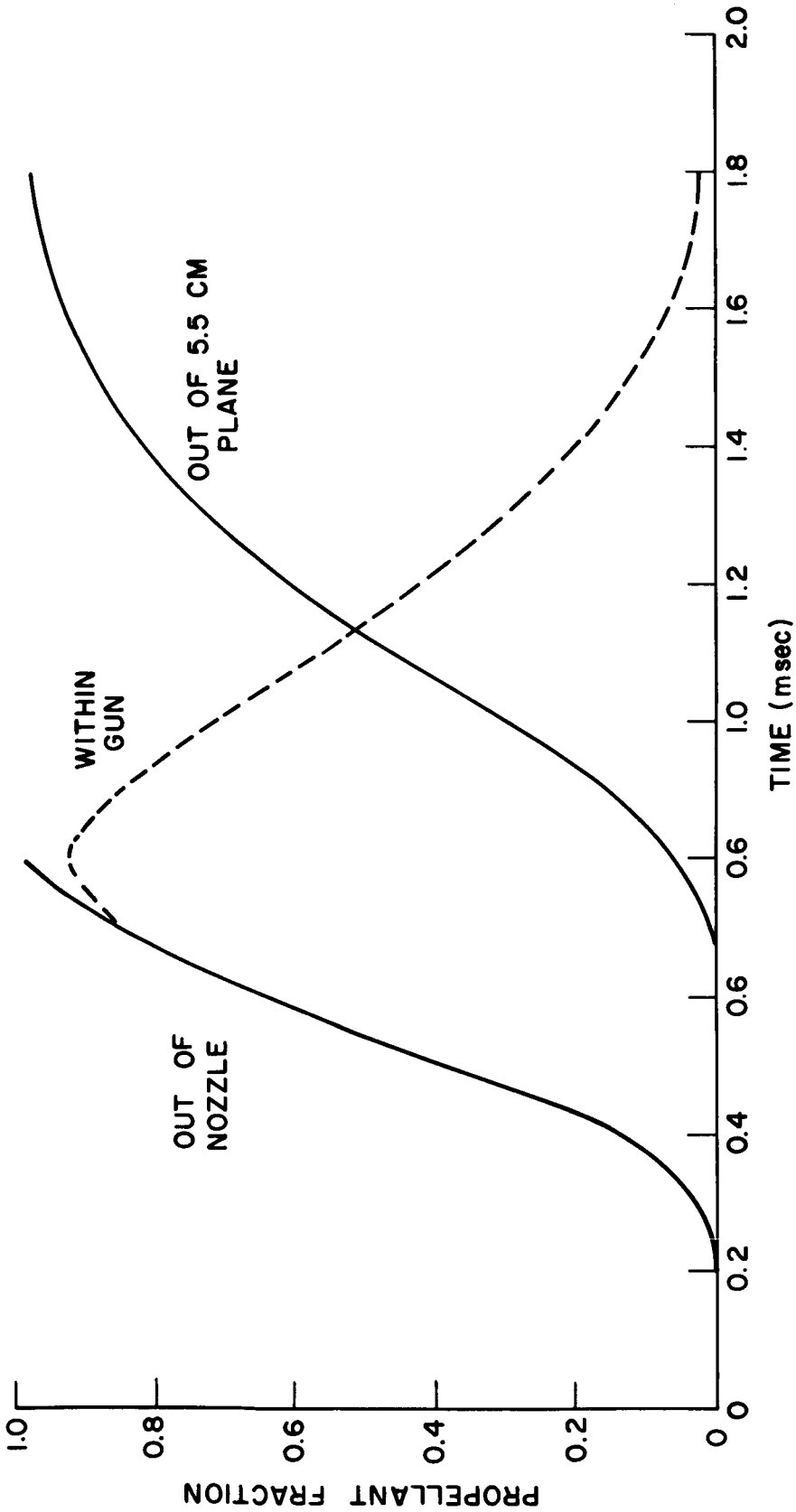

Figure 13. Propellant Fraction Between Nozzles and Plane 5.5 cm. Downstream

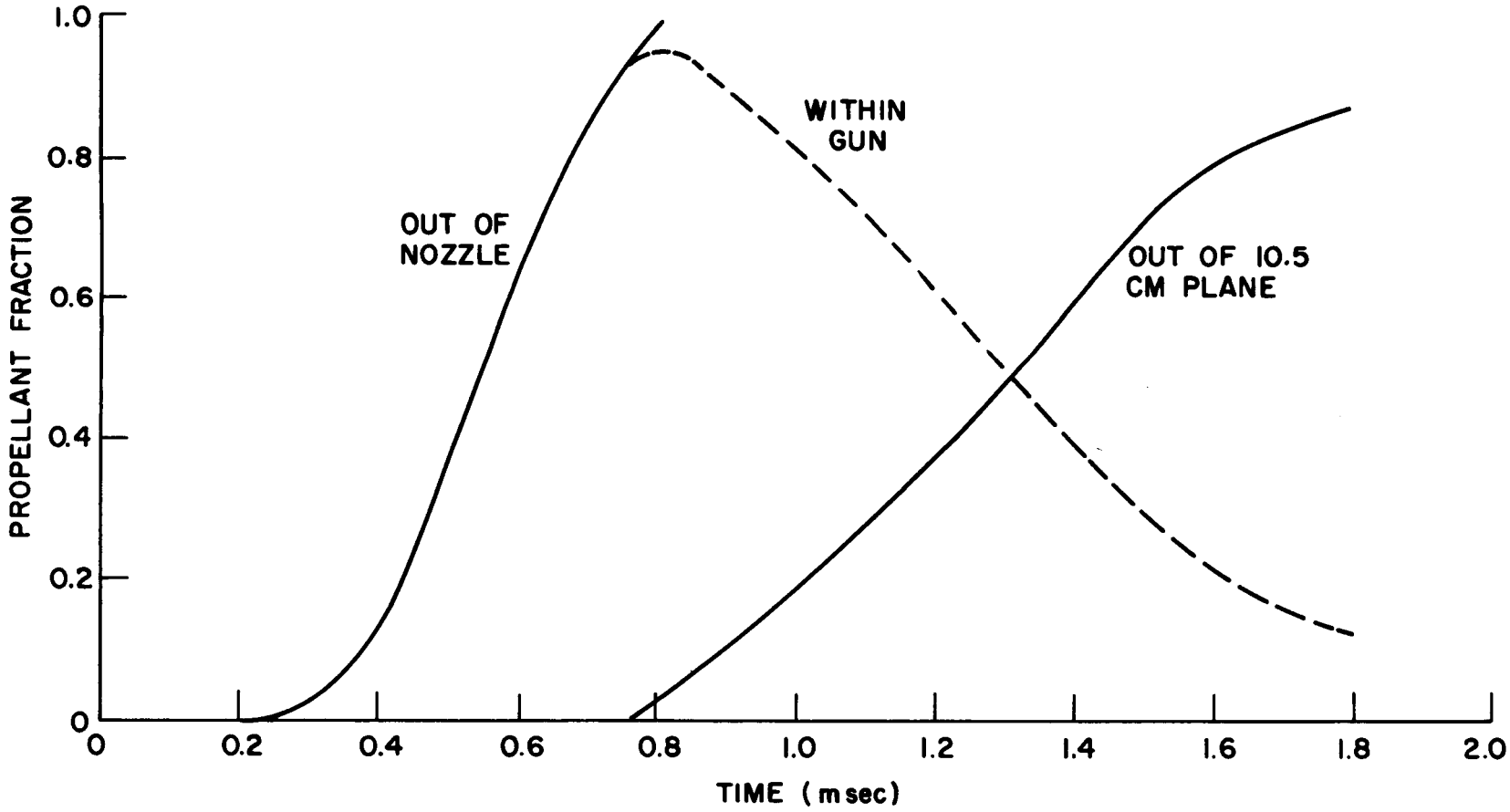

Figure 14. Propellant Fraction Between Nozzles and Plane 10.5 cm. Downstream

Within the uncertainties of the measurement, the maximum propellant fraction within the gun occurrs near 0.8 milliseconds for all three cases. The only difference lies in the value of this maximum fraction. Even this peak value does not vary much, however, and is over 90% in any case.

The type of propellant density distribution that exists in this region beyond the gun muzzle is indicated by the isobars shown on Figures 15 through 19. The form of a flat density front is approached at distances 15 cm beyond the muzzle, while closer in the stream type of profile still dominates. The progress of the gas away from the gun can be traced very clearly here.

3.4 Summary and Conclusions Regarding Propellant Distribution

Gas density measurements have shown that the propellant injected by the new ball valve emerges in a well-defined axial stream that fills the rest of the gun through sidewards expansion. This leads to more gentle pressure gradients within the gun than had heretofore been observed. Since the main gas stream no longer intercepts the outer electrode the arrival of the isobar that self-triggers the discharge is delayed and the self-triggering time is extended to .55 to .65 milliseconds. In addition, the total amount of propellant that must be injected so that the gun will self-trigger is also much increased, once more due to the new direction of the propellant stream.

The detailed effects of this completely new pre-fire propellant distribution have not yet been completely analyzed. Future efforts will be directed to understand all its implications and to slight modifications in the flow direction.

4. PERFORMANCE OF THE A9DB ENGINE

A water cooled calorimeter was used to determine the energy in the exhaust stream of the A9DB engine for various voltages and propellant

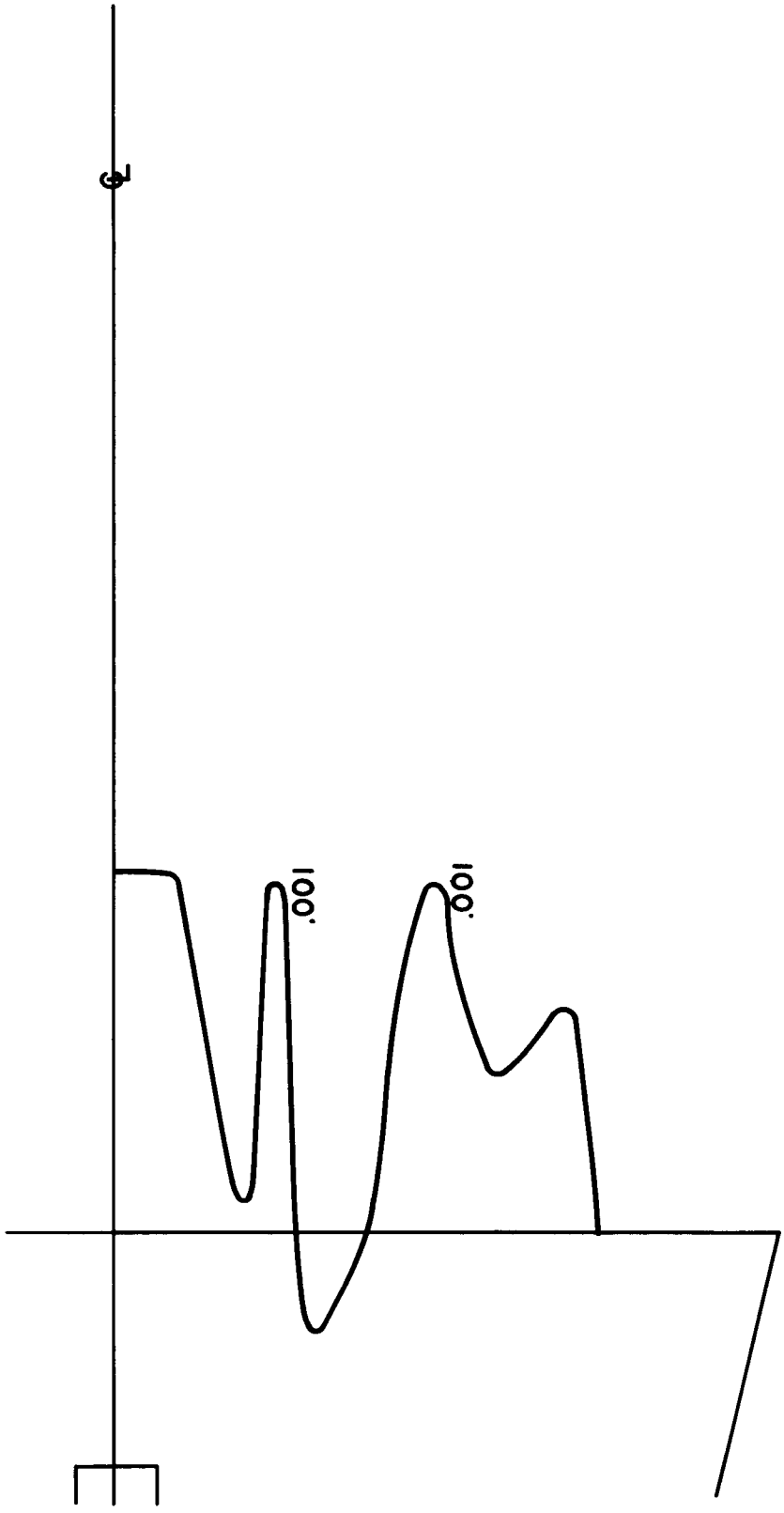

Figure 15. Isobars beyond A-8DB Gun - .5 ms.

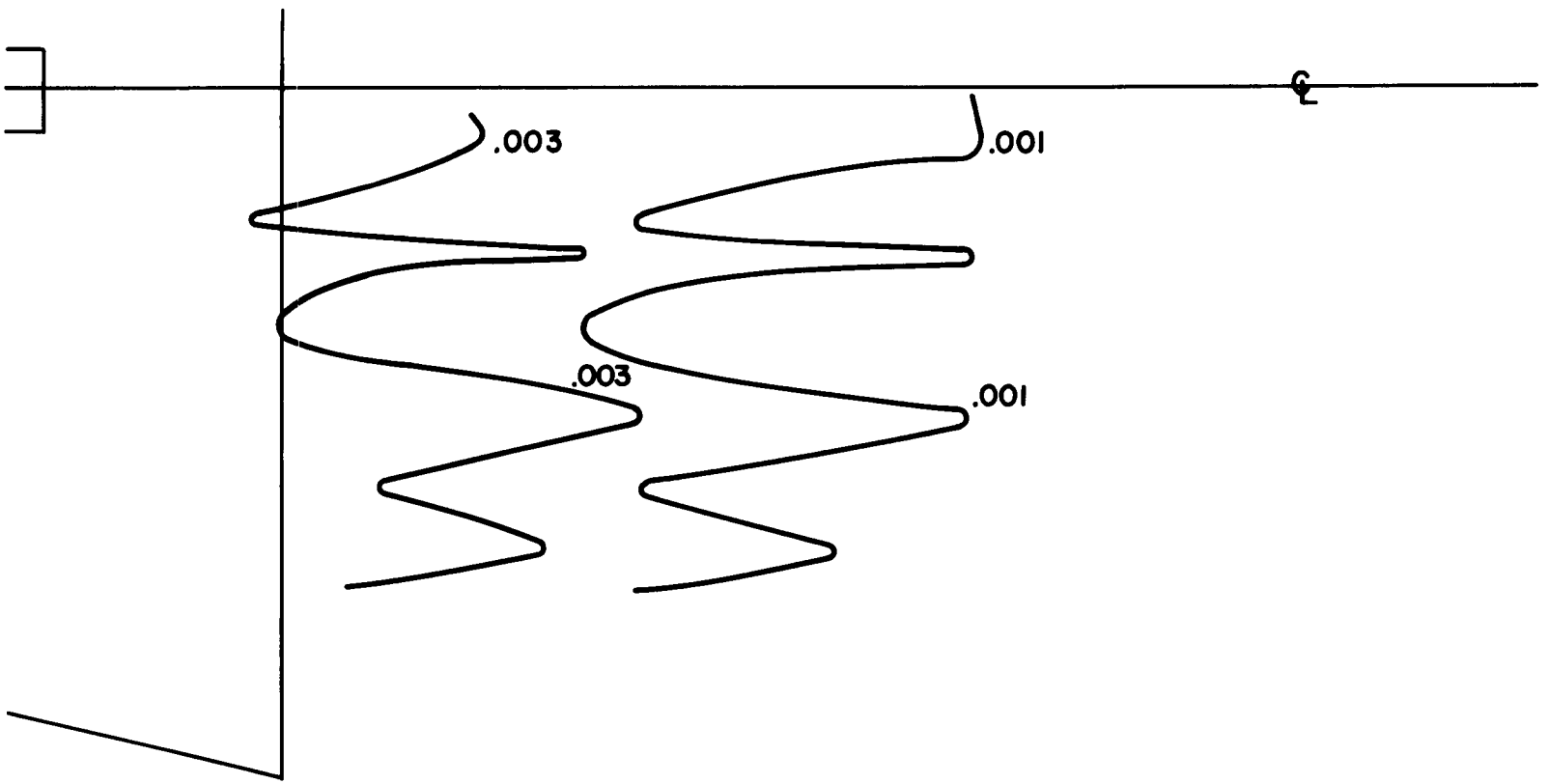

Figure 16. Isobars beyond A-8DB Gun - .6 ms.

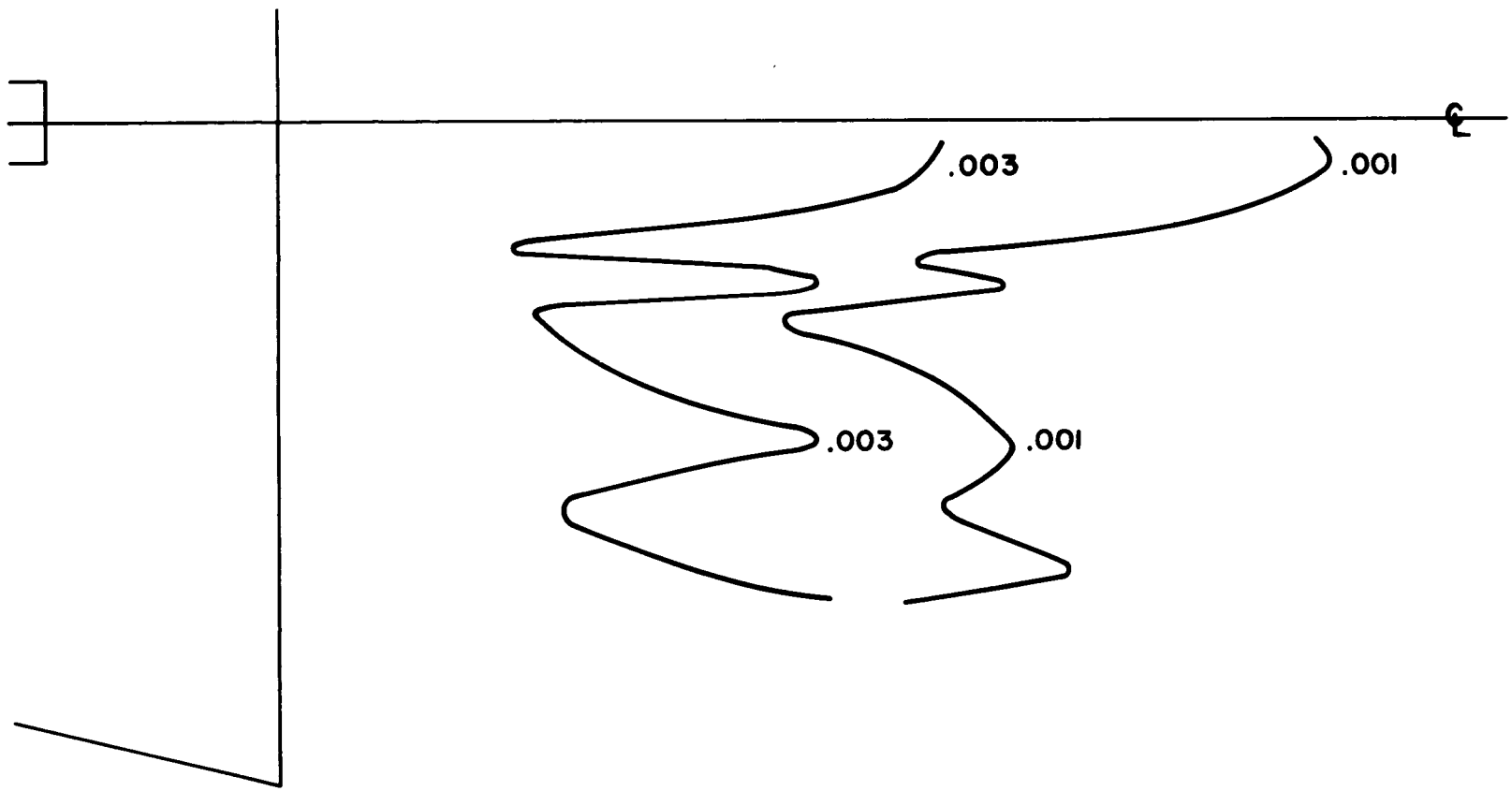

Figure 17. Isobars beyond A-8DB Gun - .7 ms.

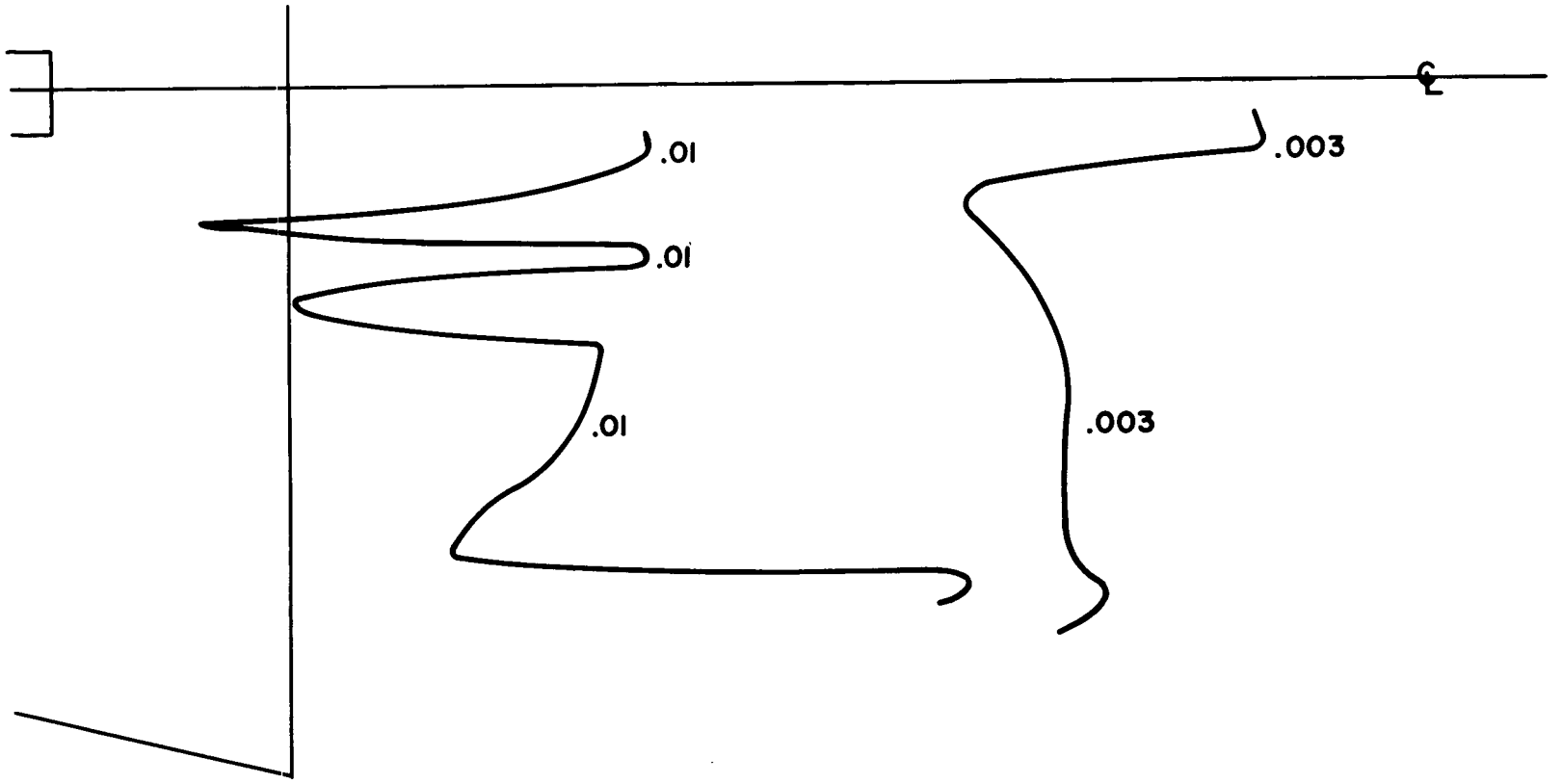

Figure 18. Isobars beyond A-8DB Gun - .8 ms.

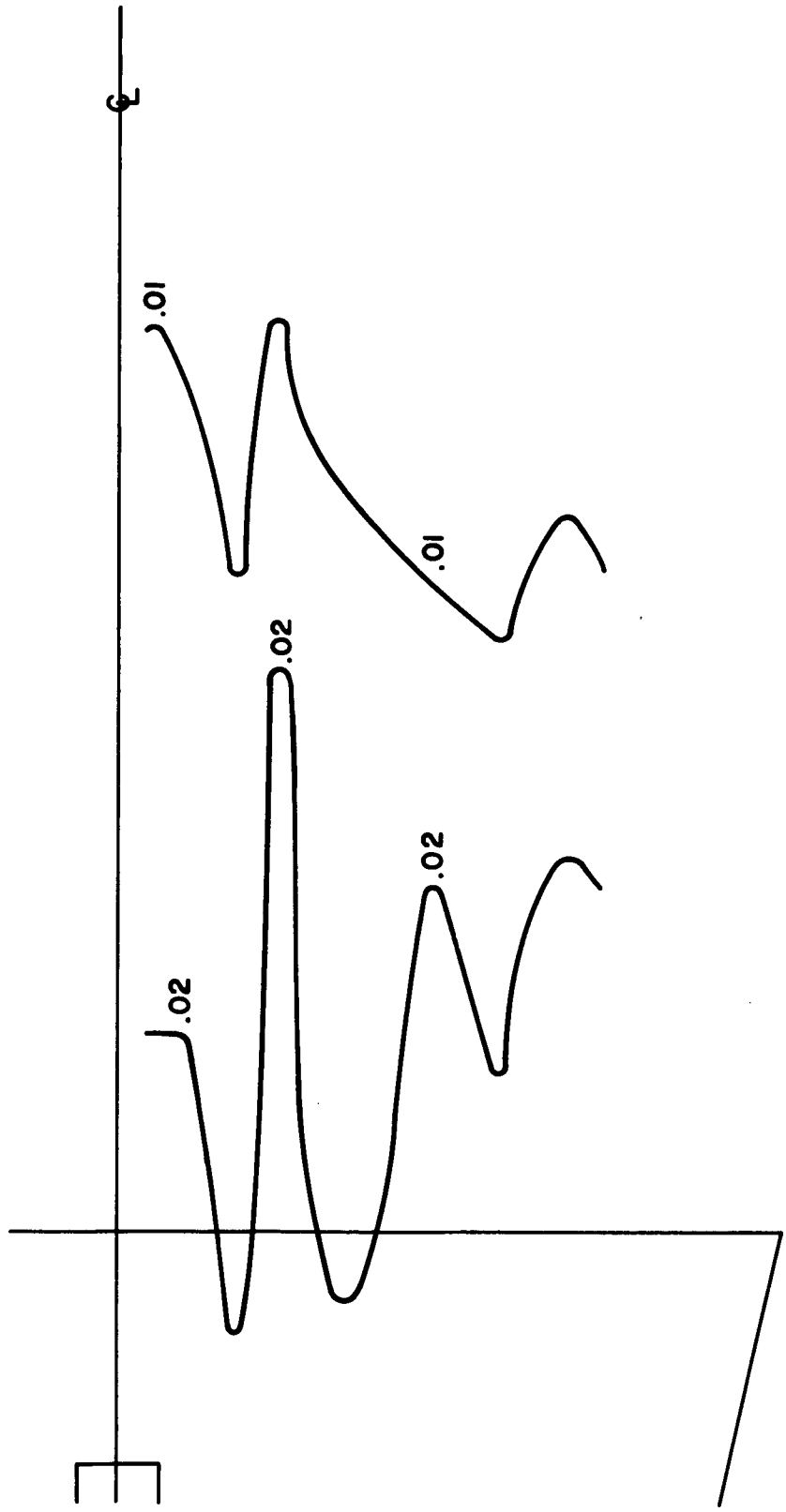

Figure 19. Isobars Isobars beyond A-8DB Gun - 1.0 ms.

mass inputs. The highest energy efficiency consistently obtained from measurements on the A9DB engine was 65% at 2 KV and a mass flow of .07 mg/sec. This efficiency, however, was found to occur under comparatively low mass flow conditions which implied undesirably high I_{sp}'s. This was confirmed by subsequent thrust and mass flow measurements at the same conditions which led to the above performance, which resulted in an overall efficiency ($T^2/2\,\dot{m}\,P$) of 61% at an I_{sp} of 12,000 sec. Under self-triggered operation with a larger mass flow, an efficiency of 35% at an I_{sp} of 5400 sec. was measured. Thus, the requirement for injecting more mass prior to the controlled triggering of the discharge had not been entirely solved by use of the ball valve seat in the "wide-open" A9D configuration. The A8DB, with additional nozzles ahead of the valve seat to provide augmented directivity of the flow, offered the possibility of increasing the performance.

5. PERFORMANCE OF THE A-8DB ENGINE

Subsequent installation and operation of the ball valve assembly in the A-8DB gun permitted more than twice the amount of propellant to be injected into this geometry, short of self-triggering, than could be injected into the A-9DB gun. In the A-8DB gun, the effect of increasing the propellant input was a relatively small increase in thrust level which was insufficient to prevent a decrease in overall efficiency at a given I_{sp}. Thrust vs. mass flow for representative intervals between valve actuation and discharge initiation are shown in Figure 20. Overall efficiency vs. I_{sp} at several mass flows and discharge delay times are shown in Figure 21.

The peak calorimeter measured efficiency for the A-8DB gun, found also at the lowest propellant flow rates used, was 77%. It should be stated here that this figure should not be directly compared to the performance of the A-9DB gun since the A-9DB data were obtained prior

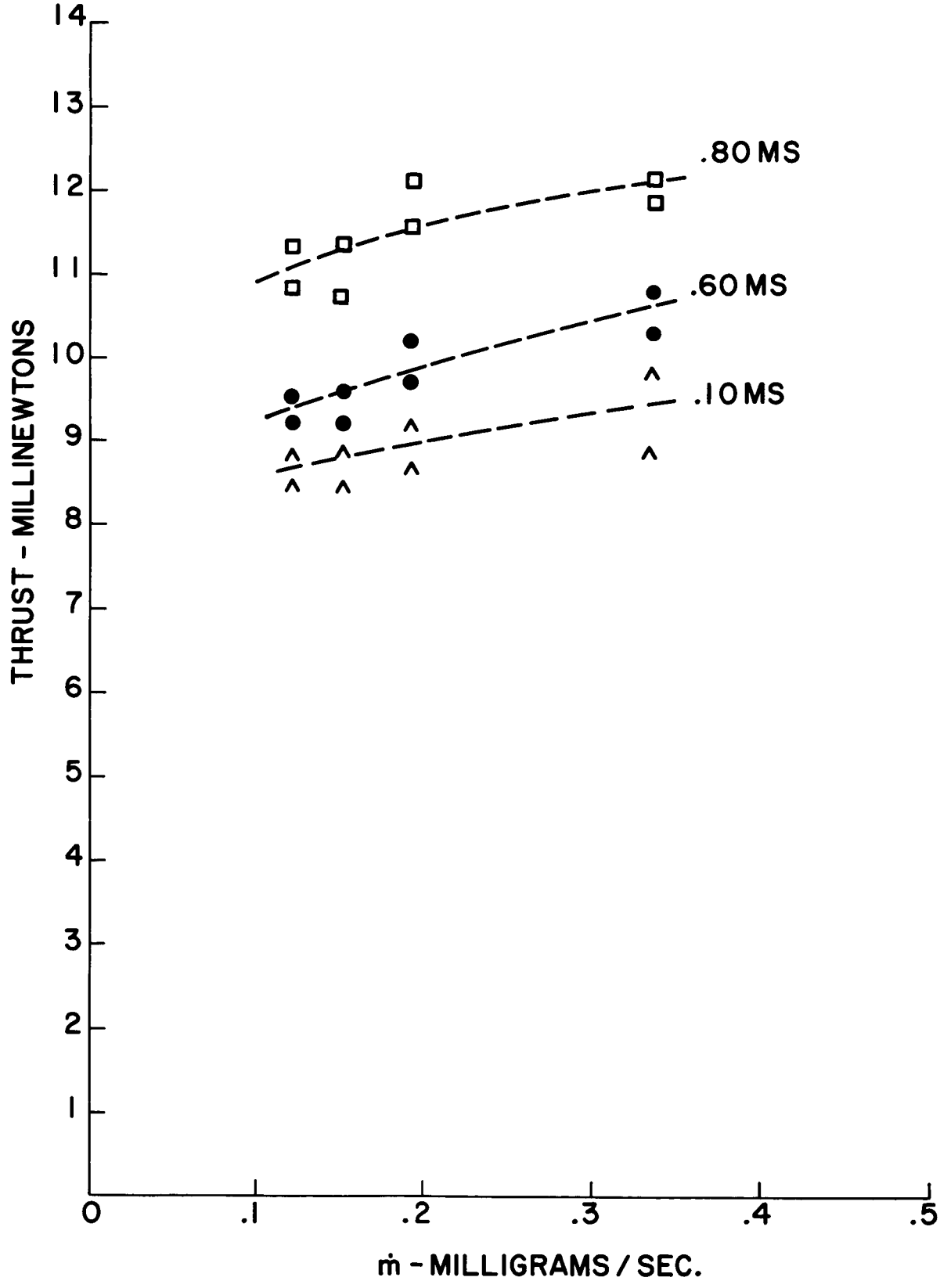

Figure 20. Thrust vs. Mass Flow for Various Delays - A-8DB Gun

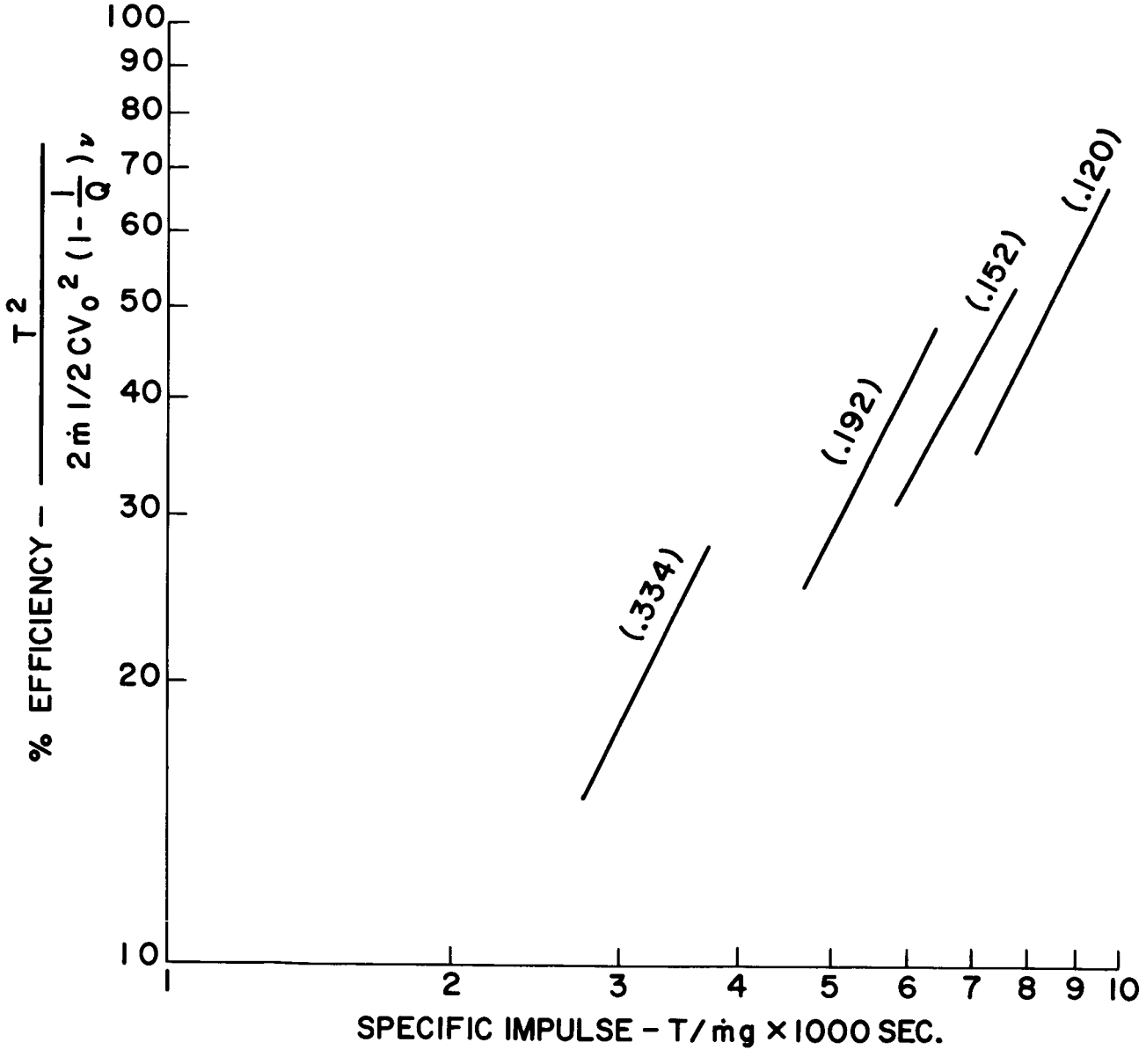

Figure 21. η_o vs. I_{sp} - A-8DB Gun

to the installation of the higher Q capacitor bank described in section 2. The energy efficiency of the A-8DB with the lower Q bank had been 72%. As has been pointed out that the reason for the increase from 72% - 77% is yet to be determined.

6. PERFORMANCE OF THE A-7D WITH THE HIGHER Q CAPACITOR BANK

Since the performance of the A-7D gun using the disc valve was comparable to that of the A-8D and subsequent A-8DB guns, it was deemed desirable to redetermine this performance with the new higher Q capacitor bank, first, at a capacitance close to the original 45 μfd and later at higher capacitance values. The results of thrust and mass flow data on this gun at 42.5 mfd are presented below. Thrust vs. mass flow data are shown in Figure 22 and overall efficiency vs. I_{sp} are shown in Figure 23.

7. GRIDDED PROBE MEASUREMENTS

Gridded probe measurements have been made with a new version of the multi-gridded electrostatic probe. Due to difficulties with the high voltages, required stopping potential data have not been obtained with xenon. Such data have been obtained with nitrogen, however.

The analysis for the interpretation of these data is here included. In order to obtain the distribution function, first note that the number of ions per second is given by

$$\frac{dn}{dt} = \frac{I}{ne} \tag{6.1}$$

where I is the ion current, and n is the number of charges per ion. The particle flow rate may be related to the velocity by the following equation:

$$\frac{dn}{dt} = \frac{dn}{dV}\,\frac{dV}{dt}\ , \tag{6.2}$$

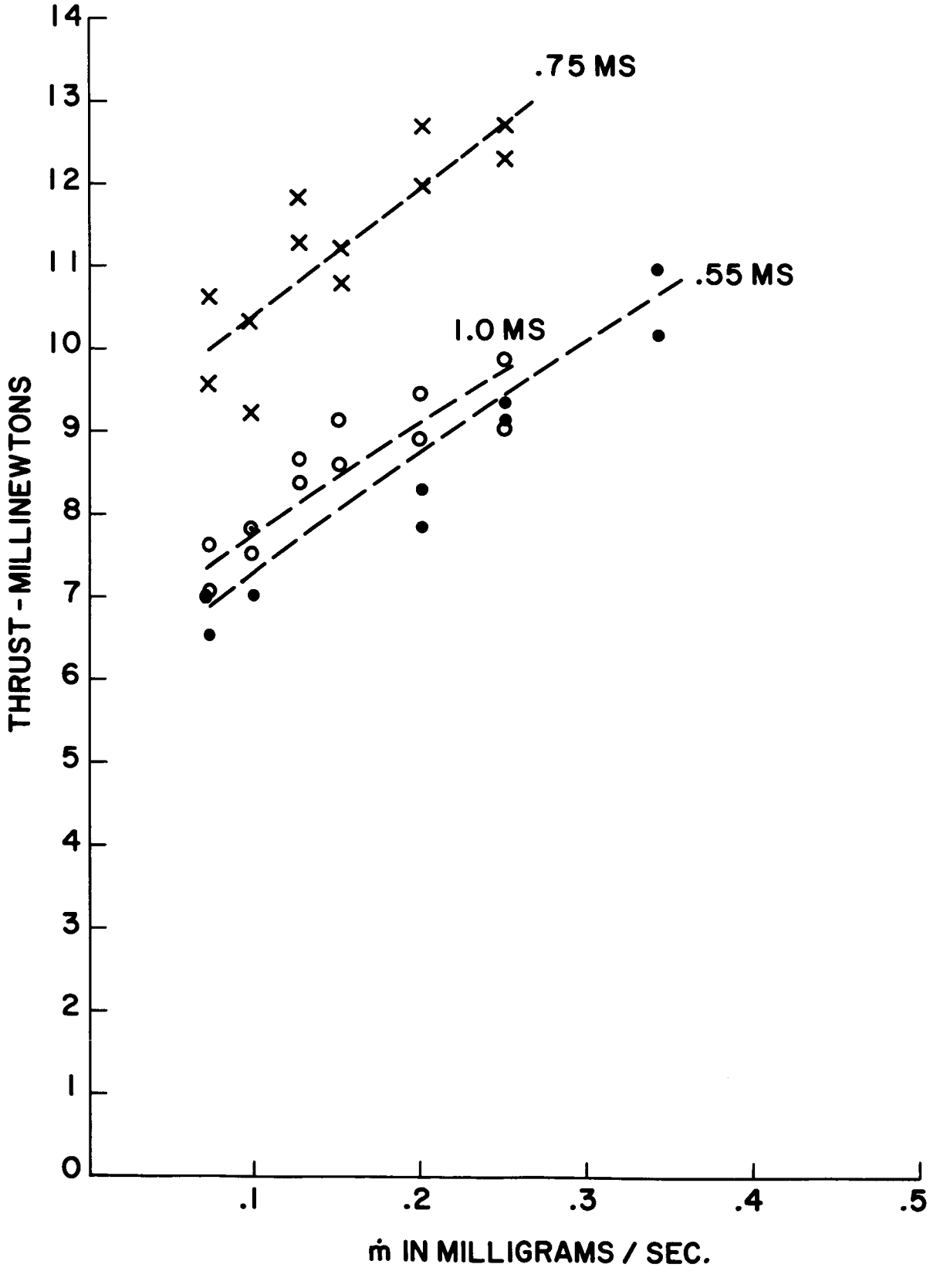

Figure 22. Thrust vs. Mass Flow A-7D Gun

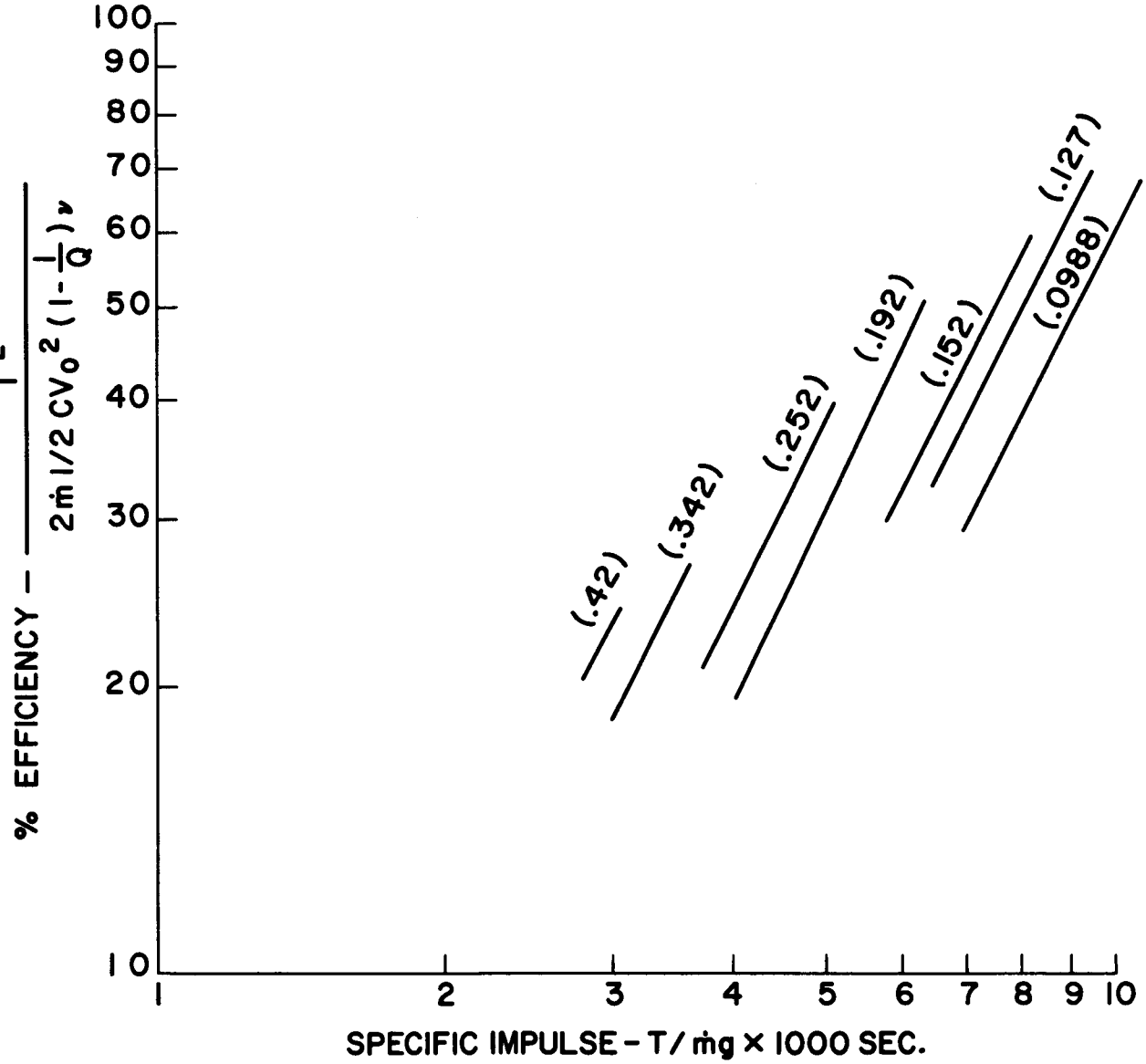

Figure 23. η_o vs. I_{sp} - A-7D Gun

where V is the velocity. When d is the distance to the probe,

$$\frac{dV}{dt} = -\frac{2d}{t^2} \tag{6.3}$$

Then, the velocity distribution is given by:

$$\frac{dn}{dV} = \frac{I}{ne}\,\frac{t^2}{2d} \quad . \tag{6.4}$$

The average I_{sp} can be determined from the expression

$$\bar{I}_{sp} = \frac{\int \frac{V}{g}\,\frac{dn}{dV}\,\delta V}{\int \frac{dn}{dV}\,\delta V}$$

Using the above expressions for dn/dV and dV, this becomes

$$\bar{I}_{sp} = \frac{\int \frac{V}{g}\,\frac{I\,t^2}{2ned}\,\frac{2d}{t^2}\,\delta t}{\int \frac{I\,t^2}{2ned}\,\frac{2d}{t^2}\,\delta t}$$

Since V = d/t

$$\bar{I}_{sp} = \frac{\int \frac{d}{g}\,\frac{I}{nt}\,\delta t}{\int \frac{I}{n}\,\delta t} \quad .$$

Note that the degree of ionization of the ions as a function of time (velocity) must be known. If the bulk of the ions are singly ionized, the n drops out of this expression. However, an accurate $\bar{I}_{sp}$ determination requires the application of the above equation to a dn/dV vs. t plot as extracted from stopping potential data. In this way, multiply ionized species may be easily identified and appropriately weighed.

A sample of the information thus obtained with nitrogen is shown in Figure 24. This represents the velocity distribution of the bulk of the ions collected by the probe. Note that doubly and triply ionized

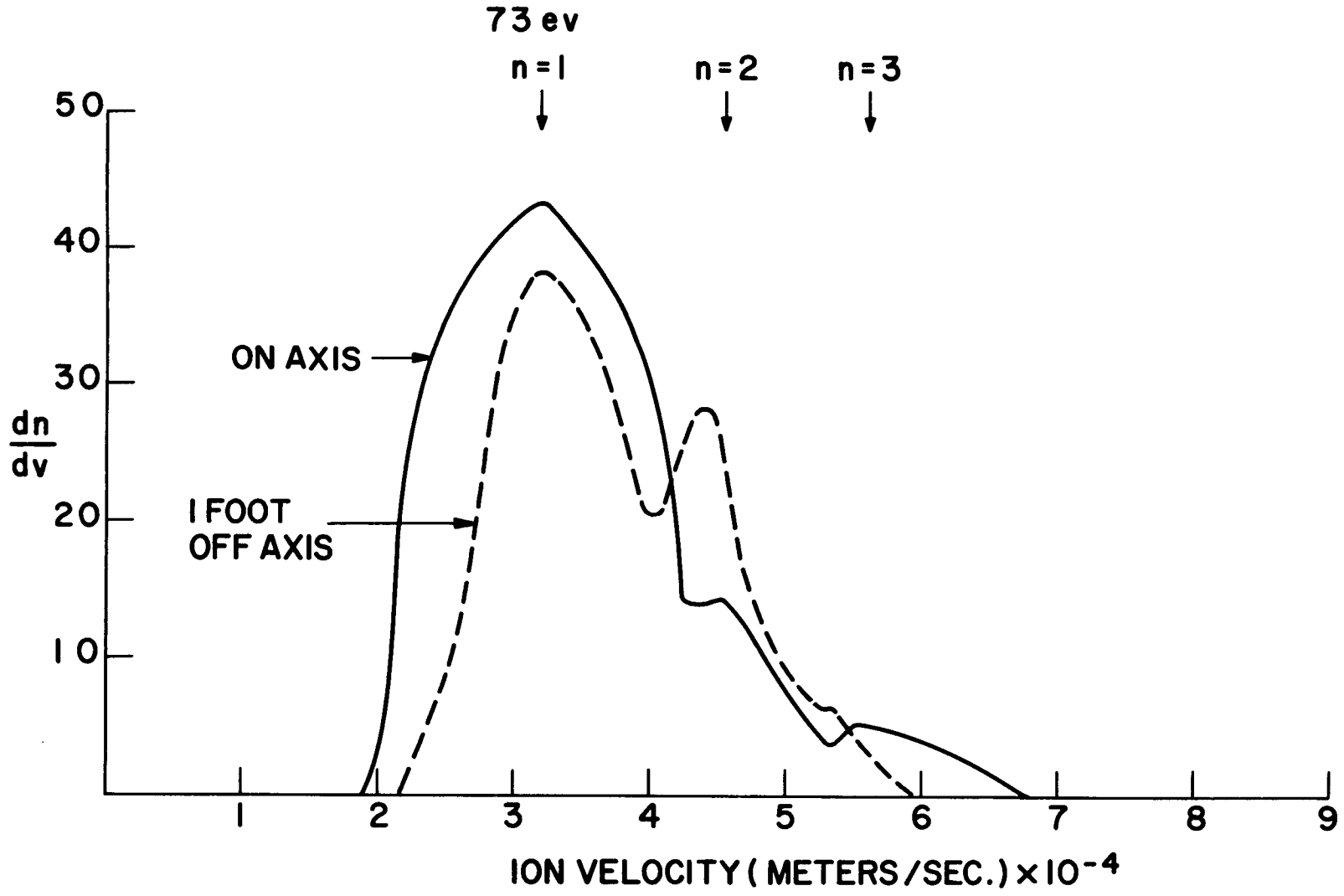

Figure 24. Velocity Distribution of Particles in A-7D Gun at 2 KV

nitrogen species (n = 2, n = 3) represent only a small fraction of the exhaust.

Thrust and mass flow measurements obtained under the same conditions give an over-all efficiency of about 20% at 3,100 seconds. If the I_{sp} is corrected for the amount of gas actually within the gun at the time of firing ($\sim$ 70% from the third quarterly report), the average ion velocity one should expect is 4.4×10^4 m/sec. A rough determination of the average ion velocity, taking into consideration all the points mentioned earlier, gives a value of about 4.75×10^4 m/sec.

Similar confirmation has been seen on several other runs, including when the probe is placed in an off-axis position.

8. SUMMARY AND CONCLUSIONS REGARDING ENGINE PERFORMANCE

It is apparent that the performance of the A-7D gun is not significantly different from that of the A-8DB configuration even though the propellant distribution has been altered. There are several possible reasons for the lack of improvement in overall efficiency at a given I_{sp}.

(1) The first attempt at optimizing the propellant distribution using the spherical valve seat in the particular configuration described above may not have been successful. Redirection of the propellant stream may be necessary.

(2) A mechanical problem occurring occasionally in the use of the spherical seat may be responsible for an undesirable alteration of the propellant input. At times the amount of propellant required to self-trigger the gun would drop to very low values. This was interpreted as being a result of uneven opening of the valve which would lead not only to the lower mass flows for self-triggering but a non-uniform distribution of the propellant which was injected. This irregularity was not disclosed by the gas density probe measurements, probably because these measurements are made on a single shot basis and the total number of shots expended is less than a minute of repetitive operation. Improved design of

the valve opening mechanism could in itself lead to improved performance.

(3) Some limit in performance has been reached for this particular combination of electrical characteristics, particularly voltage and capacitance as matched to the propellant input. The most obvious opportunity for improvement rests in an increase in the capacitance of the energy storage bank. The trend to increased efficiency with increasing capacitance has been observed previously and not followed beyond 45 μfd. It may be of even greater importance to increase the capacitance for the present gun length when using xenon rather than nitrogen, since the gun length had been chosen as optimum for 45 mfd using nitrogen and the per particle mass of xenon is much greater than that of nitrogen.

In the present set of measurements, a trend towards increased η_o, at a given I_{sp}, with increase in the available energy per discharge has been noted. We have been prevented from following this trend to a satisfactory operating point, as capacitor voltage is increased, by the fact that self-triggering sets in before an optimum condition has been reached. We hope to pursue this trend further in the next period with the expedient of increasing the available energy per discharge with an increase of capacitance, thus avoiding the premature self-triggering observed at the higher voltages. Whether such a change can increase or even maintain the coupling of energy to the plasma, must be determined by measuring the performance of the engine.